Theoretical Simulations of the Response for Circular Tubes under Cyclic Bending

Kuo-Long Lee[1], Kao-Hua Chang[2*], and Wen-Fung Pan[3]

[1] *Department of Innovative Design and Entrepreneurship Management, Far East University*
[2] *Department of Mold and Die Engineering, National Kaohsiung University of Applied Sciences*
[3] *Department of Engineering Science, National Cheng Kung University*

ABSTRACT

In this paper, the endochronic theory combined with the principle of virtual work and finite element analysis softwares, ANSYS and ABAQUS, are used for simulating the moment-curvature and ovalization-curvature relationships of circular tubes subjected cyclic bending. Two different sizes of the 316L stainless steel circular tubes subjected to cyclic bending are tested in this study. When compared with experimental data, it is shown that three methods lead to good simulation of the moment-curvature relationship. However, the endochronic theory combined with the principle of virtual work has the closer simulation of the ovalization-curvature response with the experimental data than the simulations by finite element analysis softwares, ANSYS and ABAQUS.

Keywords: Endochronic Theory, Principle of Virtual Work, ANSYS, ABAQUS, Cyclic Bending, Moment, Curvature, Ovalization

圓管在循環彎曲負載下行為之理論分析

李國龍[1]　張高華[2*]　潘文峰[3]

[1] 私立遠東科技大學創新設計與創業管理系
[2] 國立高雄應用科技大學模具工程系
[3] 國立成功大學工程科學系

摘　　要

本文以內涵時間理論結合虛功原理、有限元素分析軟體 ANSYS 和有限元素分析軟體 ABAQUS 來描述圓管承受循環彎曲負載時的彎矩-曲率及橢圓化-曲率關係。在本研究中，兩種不同尺寸的 316L 不銹鋼圓管承受循環彎曲負載下的行為也進行實驗的測試。當與實驗結果比較後發現，三種方法皆可良好的描述彎矩-曲率的關係。然而，內涵時間理論結合虛功原理比有限元素分析軟體 ANSYS 和有限元素分析軟體 ABAQUS 所描述的橢圓化-曲率關係較接近實驗結果。

關鍵詞：內涵時間理論，虛功原理，ANSYS，ABAQUS，循環彎曲，彎矩，曲率，橢圓化

文稿收件日期 101.3.9;文稿修正後接受日期 101.10.2; *通訊作者
Manuscript received Mar. 9, 2012; revised Oct. 2, 2012; * Corresponding author

Ⅰ. INTRODUCTION

Industrial circular tubular components (such as: offshore pipelines, platforms in offshore deep water, nuclear reactors, etc.) are generally subjected to bending loads. The bending of circular tubes leads to the ovalization of the tube cross-section (the change of the outside diameter ΔD_o (= D_o-D') divides by the original outside diameter D_o as shown in Fig. 1). Reverse bending and subsequent repeated cyclic bending may cause a gradual growth in ovalization. The tube will buckle when a critical magnitude of ovalization is reached. The buckling of the tube element will cause a disaster of the entire structure. Therefore, it is of great importance to understand the response and buckling of circular tubes under cyclic bending in many industrial applications.

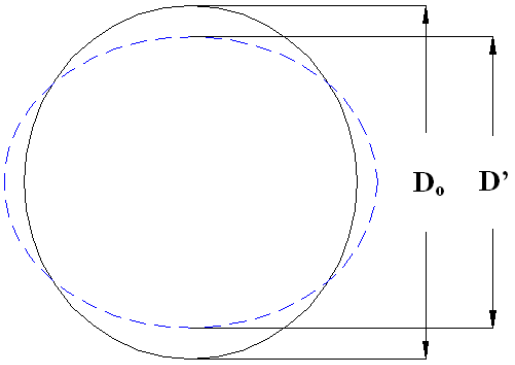

Fig. 1. The definition of ovalization

In 1982, Kyriakides and Shaw [1] first designed and constructed the tube cyclic bending machine. It was used to examine the response and stability of elastoplastic pipes under monotonic bending and external pressure. Thereafter, the bending machine has been used to investigate a series of tube materials under monotonic or cyclic bending with or without external pressure. For example: Shaw and Kyriakides [2] researched inelastic behavior of 6061-T6 aluminum and 1018 steel tubes subjected to cyclic bending; Kyriakides and Shaw [3] extended the analysis of 6061-T6 aluminum and 1018 steel tubes to the stability conditions under cyclic bending; Corona and Kyriakides [4] investigated the stability of 304 stainless steel tubes subjected to combined bending and external pressure; Corona and Kyriakides [5] studied the degradation and buckling of 6061-T6 aluminum and 1020 carbon steel tubes under cyclic bending and external pressure; Corona and Vaze [6] studied the buckling and collapse of thin-walled seamless steel square tubes under bending; Vaze and Corona [7] experimentally investigated the elastic-plastic degradation and collapse of steel tubes with square cross-sections under cyclic bending; Kyriakides and Lee [8] investigated the lowest pressure at which confined collapse can propagate in confined steel tubes; Corona et al. [9] used a set of bending experiments conducted on aluminum alloy tubes to investigating the yield anisotropy effects on the buckling; Kyriakides et al. [10] studied the plastic bending of steel tubes with diameter- to-thickness ratio (D_o/t ratio) of 18.8 for exhibiting Lüders bands through their experiment; Sakakibara et al. [11] studied the effect of internal corrosion or erosion defects on the collapse of pipelines under external pressure.

In 1998, Pan et al. [12] designed and set up a new measurement apparatus. It was used with the cyclic bending machine to study various kinds of tubes under different cyclic bending conditions. For instance: Pan and Fan [13] studied the effect of the prior curvature-rate at the preloading stage on the subsequent creep (moment is kept constant for a period of time) or relaxation (curvature is kept constant for a period of time) behavior; Pan and Her [14] investigated the response and stability of 304 stainless steel tubes subjected to cyclic bending with different curvature-rates; Lee et al. [15] studied the influence of the D_o/t ratio on the response and stability of circular tubes subjected to symmetrical cyclic bending; Lee et al. [16] experimentally explored the effect of the D_o/t ratio and curvature-rate on the response and stability of circular tubes subjected to cyclic bending; Chang et al. [17] studied the influence of the mean moment effect on circular thin-walled tubes under cyclic bending; Chang and Pan [18] discussed the buckling life estimation of circular tubes subjected to cyclic bending.

In this paper, the mechanical behavior of circular tube under cyclic bending is theoretically studied. Experimental data of the moment-curvature and ovalization-curvature responses of 316L stainless steel tubes under

cyclic bending are used for comparison. Three different analysis methods, the endochronic theory combined with the principle of virtual work, finite element software ANSYS and finite element software ABAQUS, are included. It is shown that the three analysis methods lead to good simulation of moment-curvature relationship. However, the endochronic theory combined with the principle of virtual work has the best simulation of the ovalization-curvature response when compared with the experimental data and the simulations by ANSYS and ABAQUS.

Ⅱ. EXPERIMENTAL FACILITY, MATERIALS, SPECIMENS AND TEST PROCEDURES

In this study, the cyclic bending experiments on 316L stainless steel tubes are conducted using a tube-bending device and a curvature-ovalization measurement apparatus. Detailed descriptions of the device, apparatus, materials and test procedures are stated in the following.

2.1 Tube-bending device

A schematic drawing of the tube-bending device is shown in Fig. 2. It is designed as a four-point bending machine, capable of applying reverse cyclic bending. The device consists of two rotating sprockets resting on two support beams. Heavy chains run around the sprockets resting on two heavily supported beams 1.25 m apart. This allows the maximum length of test specimen to be 1 m. The bending capacity of the machine is 5300 N-m. Each tube is tested and fitted with a solid rod extension. The contact between the tube and the rollers is free to move along the axial direction during bending. The load transfer to the test specimen is formed by concentrated loads from two of the rollers in the form of a couple. Once either the top or bottom cylinder is contracted, the sprockets are rotated, and pure bending of the test specimen is achieved. Reverse bending can be achieved by reversing the flow direction in the hydraulic circuit [2-3, 12-14].

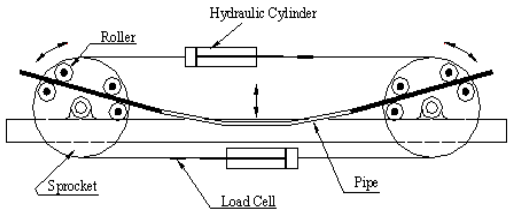

Fig. 2. Schematic drawing of the tube- bending device

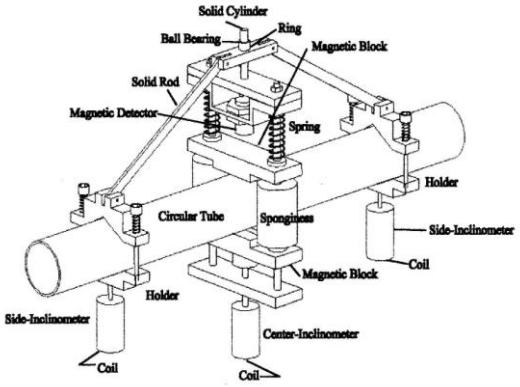

Fig. 3. Schematic drawing of the COMA

2.2 Curvature-ovalization measurement apparatus (COMA)

The COMA is an instrument used for measuring the tube curvature and ovalization of a tube cross-section. Fig. 3 shows a schematic drawing of COMA. It is a lightweight instrument, which can be mounted close to the tube mid-span. There are three inclinometers in the COMA. Two inclinometers are fixed on two holders, which are denoted as side-inclinometers (see Fig. 3). These holders are fixed on the circular tube before the test begins. Based on the fixed distance between the two side-inclinometers and the angle changes detected by the two side-inclinometers, the tube curvature can be obtained by simple calculation. In addition, by using the magnetic detector on the middle part of COMA to measure the change of outside diameter, the ovalization of the tube cross-section can be determined. A detailed description of the tube-bending device and the COMA can be found in Pan et al. [12].

2.3 Material

Circular tubes made of 316L stainless steel is used in this study. The tube's chemical composition (in mass percentages) is Cr (17.51%), Ni (12.88%), Mn (1.66%), Si (0.43%), …., and the remainder Fe. The 0.2% proof stress was 281 MPa, and its ultimate tensile stress was 583 MPa with a 62% percent elongation.

2.4 Specimens

There are two different sizes of the 316L stainless steel tubes for this test as shown in Fig. 4. One is the outside diameter of 36.3 mm and wall-thickness of 0.6 mm which is denoted as "Tube A". The other is the outside diameter of 27.2 mm and wall-thickness of 0.5 mm which is denoted as "Tube B".

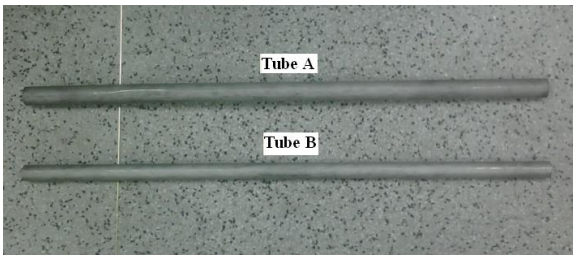

Fig. 4. A Picture of "Tube A" and "Tube B"

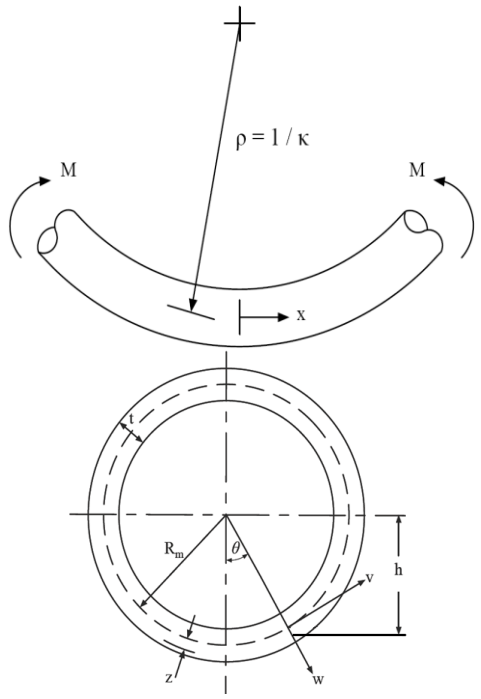

Fig. 5. Problem geometry of circular tube subjected to pure bending

2.5 Experimental procedure

In this study, cyclic bending test is conducted by using the tube-bending device. The experiment is the curvature-controlled cyclic bending test. The magnitude of the curvature is controlled and measured by COMA, which also measured the ovalization of tube cross-section. The bending moment can be calculated from the signals detected by the two load cells mounted on the tube-bending device.

Ⅲ. ENDOCHRONIC THEORY COMBINED WITH PRINCIPLE OF VIRTUAL WORK

In this section, the kinematics of the tube cross section, the constitutive model and the principle of virtual work are discussed separately.

3.1 Kinematics

A circular tube subjected to cyclic bending is considered in this study. Fig. 5 shows the problem geometry, in which R_m is the mean radius, and t is the wall thickness. Based on the axial, circumferential, and radial coordinates x, θ and r, the displacements of a point on the tube's mid-surface are denoted as *u*, *v* and *w*, respectively.

The kinematic relations required must be general enough to accommodate ovalization of the cross-section. Such a set of relations has been developed by Gellin [19] and used successfully by Kyriakides and Shaw [1]. Briefly, it is assumed that the plane sections perpendicular to the tube mid-surfaces before and during deformation. The strains are assumed to remain small but finite rotations about both axes of bending are allowed. The axial strain is expressed as (Kyriakides and Shaw [1], Shaw and Kyriakides [2]):

$$\varepsilon_x = \varepsilon_x^0 + h \cdot \kappa \tag{1}$$

and

$$h = (R_m + w)\cos\theta - v\sin\theta + Z\cos\theta \tag{2}$$

where ε_x^0 is the axial strain of the cylinder's axis, h is distance between the point and the horizontal plane passing through the center of the cross-section, κ is the tube curvature and Z

is the distance between the point and the midpoint surface. The circumferential strain is

$$\varepsilon_\theta = \varepsilon_\theta^0 + h\kappa_\theta \tag{3}$$

where

$$\varepsilon_\theta^0 = \frac{(v' + w)}{R_m} + \frac{1}{2}\left(\frac{v' + w}{R_m}\right)^2 + \frac{1}{2}\left(\frac{v - w'}{R_m}\right)^2 \tag{4}$$

and

$$\kappa_\theta = \left(\frac{v' - w''}{R_m^2}\right) \Bigg/ \sqrt{1 - \left(\frac{v - w'}{R_m}\right)^2}\,. \tag{5}$$

(') denotes the differentiation with respect to θ.

3.2 Endochronic constitutive equations

Based on the assumption of small deformation for homogeneous and isotropic materials, the increment of the deviatoric stress tensor $d\underset{\sim}{s}$ of the endochronic theory is given as (Valanis [20])

$$d\underset{\sim}{s} = 2\rho(0)\, d\underset{\sim}{e}^p + 2\underset{\sim}{h}(z)dz \tag{6}$$

and

$$\underset{\sim}{h}(z) = \int_0^z \frac{d\rho(z - z')}{dz}\frac{\partial \underset{\sim}{e}^p}{\partial z'} \tag{7}$$

$$d\underset{\sim}{e}^p = d\underset{\sim}{e} - \frac{d\underset{\sim}{s}}{2\mu_0} \tag{8}$$

where $\underset{\sim}{e}$ denotes the deviatoric strain tensor, and μ_o is the elastic shear modulus. The intrinsic time measure ζ is

$$d\zeta = \left\| d\underset{\sim}{e}^p \right\| \tag{9}$$

in which ||·|| represents the Euclidean norm. The intrinsic time scale *z* is

$$dz = \frac{d\zeta}{f(\zeta)} \tag{10}$$

where $f(\zeta)$ is a material hardening function which can be expressed as

$$f(\zeta) = 1 - Ce^{-\beta\zeta}\text{, for C < 1} \tag{11}$$

in which C and β are material parameters. If plastic incompressibility is satisfied, the elastic hydrostatic response can be written as

$$d\sigma_{kk} = 3Kd\varepsilon_{kk} \tag{12}$$

where σ_{kk} and ε_{kk} are the traces of stress and strain tensors, respectively, and *K* is the elastic bulk modulus. According to the mathematical characteristic of the kernel function ρ(z), Equation (6) is expressed as (Pan et al. [21]; Pan and Chern [22]):

$$d\underset{\sim}{s} = \sum_{i=1}^n d\underset{\sim i}{s} = 2\sum_{i=1}^n C_i\, d\underset{\sim}{e}^p - \sum_{i=1}^n \alpha_i \underset{\sim i}{s}\, dz \tag{13}$$

Where C_i and α_i are material constants. Substituting Eq. (8) into Eq. (13) leads to

$$d\underset{\sim}{s} = \frac{\mu_0}{\mu_0 + \sum_{i=1}^n C_i}\left[2\sum_{i=1}^n C_i\, d\underset{\sim}{e} - \sum_{i=1}^n \alpha_i \underset{\sim}{s}_i\, dz\right] \tag{14}$$

By using Eq. (12), Equation (14) can be expressed in terms of the stress and strain tensors as

$$d\underset{\sim}{\sigma} = p_1 d\underset{\sim}{\varepsilon} + p_2 d\varepsilon_{kk}\underset{\sim}{I} + p_3\sum_{i=1}^n \alpha_i\left(\underset{\sim}{\sigma} - \frac{\sigma_{kk}}{3}\underset{\sim}{I}\right)_i dz \tag{15}$$

where

$$p_1 = \frac{2\rho(0)}{1 + \frac{\rho(0)}{\mu_0}},\quad p_2 = K - \frac{2\rho(0)}{3\left(1 + \frac{\rho(0)}{\mu_0}\right)},\quad p_3 = \frac{1}{1 + \frac{\rho(0)}{\mu_0}} \tag{16}$$

3.3 Principle of virtual work

The principle of virtual work, which satisfies the equilibrium requirement, is given by

$$\int_V \sigma_{ij}\delta\varepsilon_{ij}\, dV = \delta W \tag{17}$$

where V is the volume of the material of the tube section considered, and δW is the virtual work of the external loads. For the case of a circular tube subjected to cyclic bending, the quantity of δW for the incremental loading can be expressed as

$$\int_V (\sigma_{ij} + \dot{\sigma}_{ij})\delta\dot{\varepsilon}_{ij}\, dV = 2R\int_0^\pi \int_{-t/2}^{t/2} [\hat{\sigma}_x\, \delta\dot{\varepsilon}_x]\, dT\, d\theta = 0 \tag{18}$$

where $\hat{\sigma}_x = \sigma + \sigma_x$ and $\dot{(\ )}$ denotes the increment of ( ). The in-plane displacements v and w are assumed to be symmetrical and are

approximated by the following expression (Shaw and Kyriakides [2], Kyriakides and Shaw [3]):

$$v \cong R_m \sum_{n=2}^{N} a_n \sin n\theta ,$$

$$w \cong R_m \sum_{n=0}^{N} b_n \cos n\theta \qquad (19)$$

where the number of terms N is chosen to ensure satisfactory convergence. Kyriakides and Shaw [3] investigated the sensitivity of the moment-curvature and ovalization-curvature response for monotonic pure bending to the number of expansion terms used in Eq. (19). Those equations clearly indicate that N = 4 or 6 is sufficient. By substituting Eqs. (1)-(5), (19) into Eq. (18), a system of 2N+1 nonlinear algebraic equations in terms of $\dot{a}_2, \dot{a}_3, \ldots, \dot{b}_0, \dot{b}_1, \dot{b}_2, \ldots, \dot{\varepsilon}_x^0$ are determined. This system of equations is solved using the Newton-Raphson method. The iterative scheme contains nested iterations for the constitutive relations.

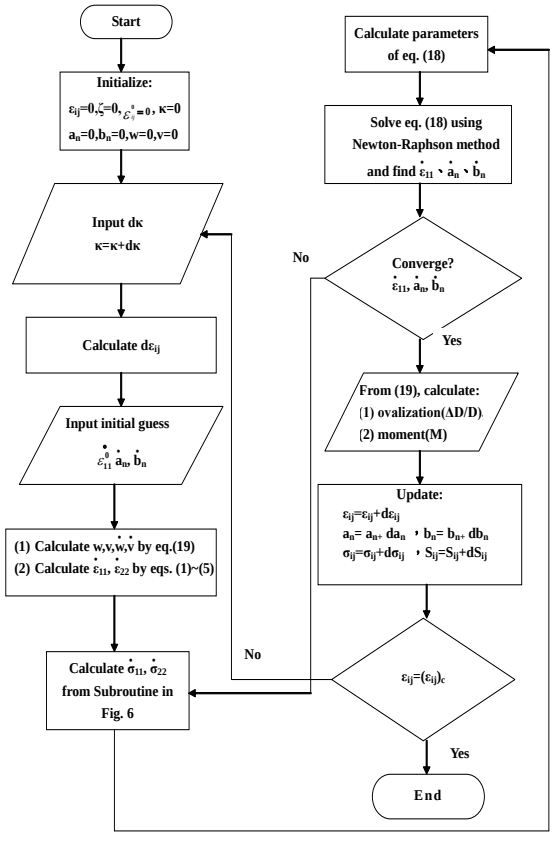

Fig. 6. Flow chart of the numerical solution procedure

Kyriakides and Shaw [3] provide a more detailed derivation of the equation system. Fig. 6 shows the main steps of the numerical solution in a flow chart. In addition, the steps of calculating the stress-strain relationship using endochronic theory are demonstrated in a flow chart in Fig. 7. When the tube subjects to bending, the stress and strain will produce in logitudinal direction (x-direction) and hoop direction (θ-direction). However, the strain and stress in radius direction (r-direction) are neglected. In the analysis of the endochronic theory combined with the principle of virtual work, x and θ dierections are 1 and 2 directions, respectively. From Eq. (19), the incremental displacement ($\dot{v}$ and $\dot{w}$) of each point on the tube's cross-section can be determined. Let's consider the values of v and w at θ = 0 and θ = π, the ovalization of the tube's cross-section is obtained.

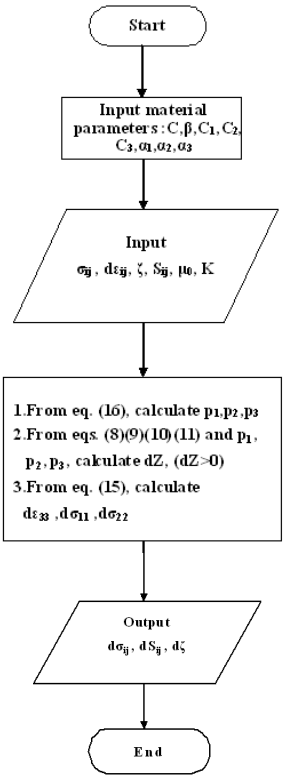

Fig. 7. Flow chart of the calculation of the endochronic theory

Ⅳ. FINITE ELEMENT ANSYS AND ABAQUS

Due to the great progress in computation speed and great improvement in the theory for

describing the elastoplastic response in finite element method in recent years, the accuracy of calculation by finite element method gets better. In this study, the finite element softwares, ANSYS and ABAQUS, are used to simulate the response of circular tube under cyclic bending.

As for the material elastoplastic behavior, the multilinear segments of the stress-strain relationship for 316L stainless steel as shown in Fig. 8 are considered in this case. The hardening rule used is the kinematic hardening rule.

Due to the symmetry of the tube, only half of the tube was considered in this analysis. Figs. 9-10 demonstrate the mesh and boundary condition of the finite element ANSYS, respectively, and Figs. 11-12 demonstrate the mesh and boundary condition of the finite element ABAQUS, respectively.

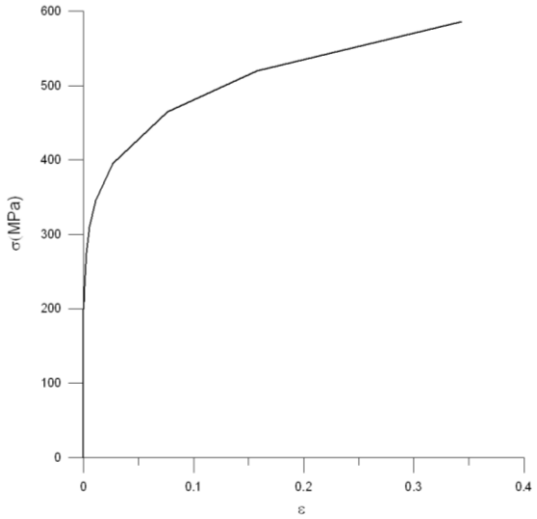

Fig. 8. Multilinear segments of the stress-strain relationship for 316L stainless steel

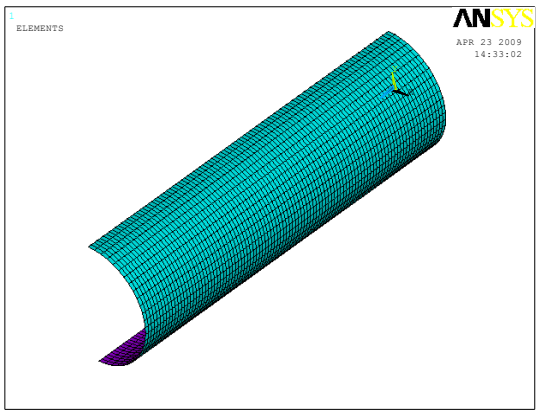

Fig. 9. Mesh of the finite element ANSYS

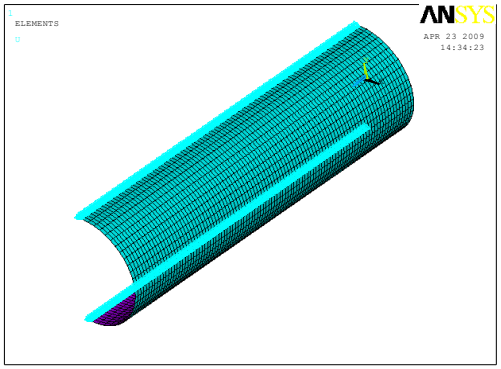

Fig. 10. Boundary condition of the finite element ANSYS

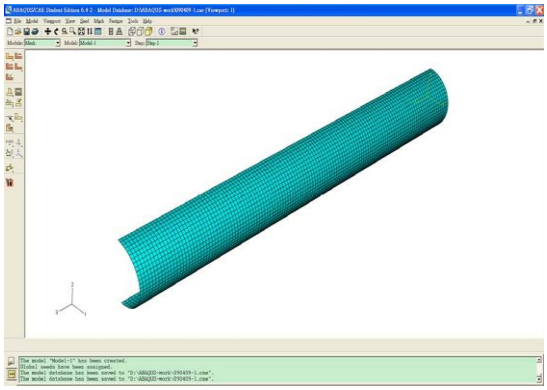

Fig. 11. Mesh of the finite element ABAQUS

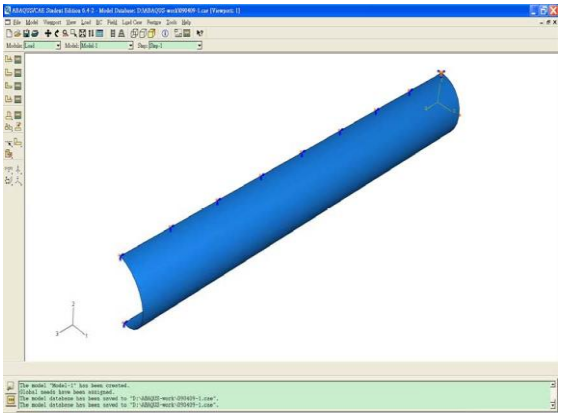

Fig. 12. Boundary condition of the finite element ABAQUS

V. EXPERIMENTAL AND THEORETICAL RESULTS

Figs. 13(a) and 13(a) show the experimental results of cyclic moment (M) - curvature (κ) curve for Tube A and Tube B, respectively. The controlled minimum and maximum values of curvature are -0.3 and 0.3

m^{-1}. It is observed from the M-κ curve that the 316L stainless steel tubes exhibit cyclic hardening and become gradually steady after a few cycles for symmetric curvature-controlled cyclic bending.

According to the method proposed by Fan [23], the material parameters for endochronic theory of 316L stainless steel are determined to be: μ_0 = 72 GPa, K = 154 GPa, $C_1 = 4.85 \times 10^5$ MPa, α_1 = 8730.4, $C_2 = 5.46 \times 10^4$ MPa, α_2 = 958.3, $C_3 = 4.7 \times 10^3$ MPa, α_3 = 168.9. Since the simulation of the M-κ behavior by the finite element method does not consider the cyclic hardening phenomenon, the endochronic theory also ignored the cyclic hardening phenomenon.Thus, the material function in the endochronic theory should be equal to one. The values of the material parameters C and β in material function are zero (Pan and Chern [23]).

Figs. 13(b), 13(c) and 13(d) show the corresponding analyses for Tube A by the endochronic theory combined with the principle of virtual work, the finite element ANSYS and the finite element ABAQUS, respectively. In general, three analyses can very well simulate the M-κ response. Similar outcome is found in Figs. 14(a)-(d) for Tube B.

Fig. 15(a) shows the experimental cyclic ovalization ($\Delta D_o/D_o$) - curvature (κ) curve for Tube A. It is shown that on first loading, the ovalization grows to a maximum value at the maximum curvature. On unloading to zero curvature, some permanent deformation of the tube cross section is observed. Continuous reverse bending to the minimum curvature causes the ovalization to increase again. The ovalization increases in a ratcheting manner with the number of bending cycles. Figs. 15(b), 15(c) and 15(d) show the corresponding analyses by the endochronic theory combined with the principle of virtual work, the finite element ANSYS and the finite element ABAQUS, respectively. It can be seen that the simulations by these three methods have some deviation from the experimental data, but the theoretical analysis by the endochronic theory combined with the principle of virtual work provides the better result when compared with the simulations by ANSYS and ABAQUS and the experimental data. Similar outcome is found in Figs. 16(a)-(d) for Tube B.

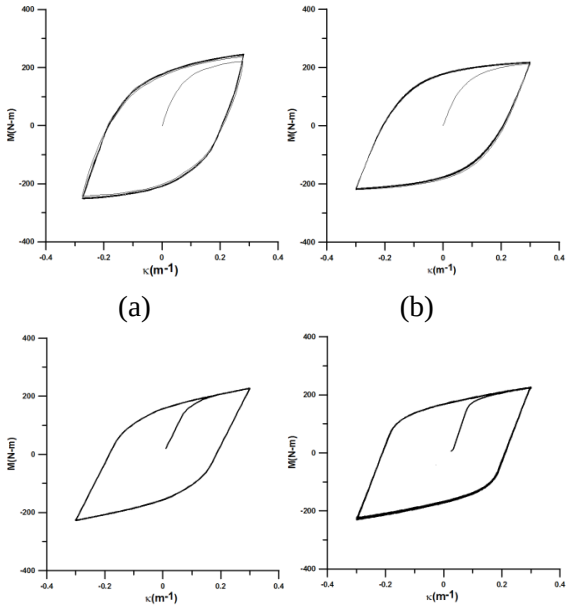

(a) (b)

(c) (d)

Fig. 13. Cyclic moment (M) - curvature (κ) for Tube A. (a) Experiment result, (b) theoretical analysis by the endochronic theory combined with the principle of virtual work, (c) theoretical analysis by ANSYS and (d) theoretical analysis by ABAQUS

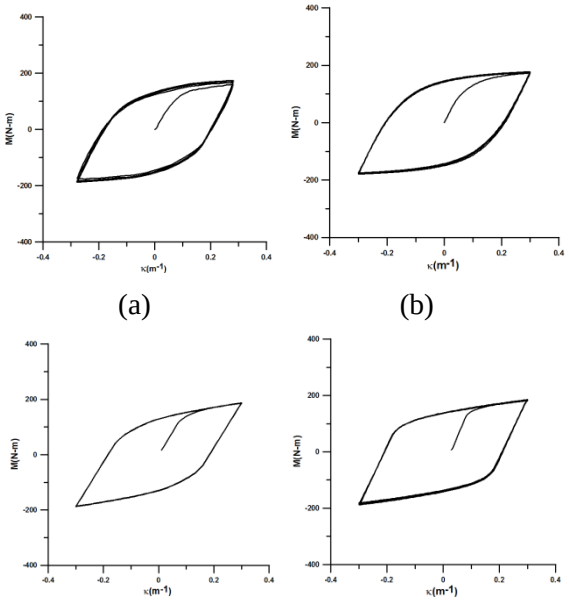

(a) (b)

(c) (d)

Fig. 14. Cyclic moment (M) - curvature (κ) for Tube B. (a) Experiment result, (b) theoretical analysis by the endochronic theory combined with the principle of virtual work, (c) theoretical analysis by ANSYS and (d) theoretical analysis by ABAQUS

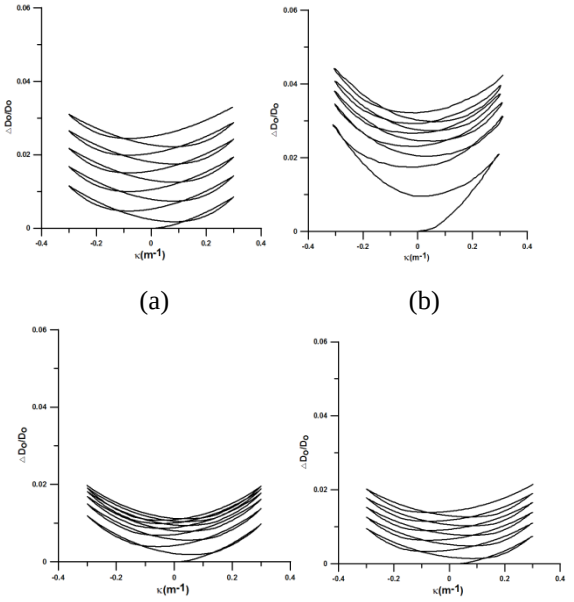

Fig. 15. Cyclic ovalization ($\Delta D_o/D_o$) - curvature (κ) for Tube A. (a) Experiment result, (b) theoretical analysis by the endochronic theory combined with the principle of virtual work, (c) theoretical analysis by ANSYS and (d) theoretical analysis by ABAQUS

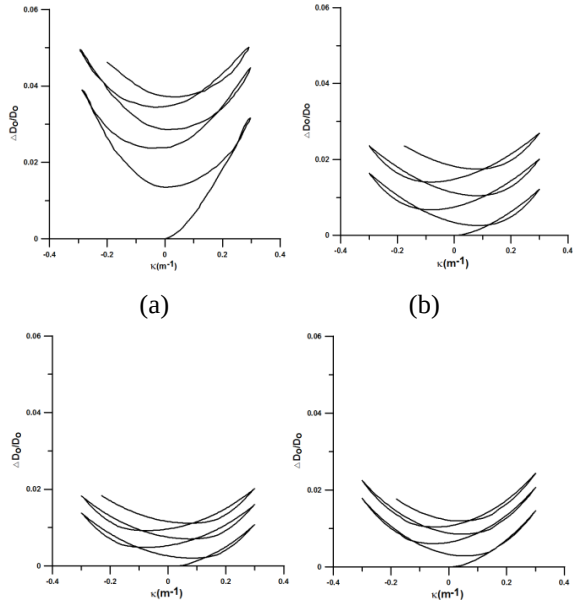

Fig. 16. Cyclic ovalization (ΔDo/Do) - curvature (κ) for Tube B. (a) Experiment result, (b) theoretical analysis by the endochronic theory combined with the principle of virtual work, (c) theoretical analysis by ANSYS and (d) theoretical analysis by ABAQUS

VI. CONCLUSIONS

In this study, the response of circular tubes is theoretically investigated. According to the experimental and theoretical results, the following important conclusions are apparent from this investigation:

(1) For symmetric curvature-controlled cyclic bending, the M – κ loop of the 316L stainless steel tube shows cyclic hardening. But the loops become gradually steady after a few cycles.

(2) For symmetric curvature-controlled cyclic bending, the $\Delta D_o/D_o$ – κ curve of the 316L stainless steel tube shows the increased ratcheting with the number of cycles. Moreover, persistent cycling eventually leads to buckling.

(3) The three analysis methods reveal a good simulation for the M-κ response. However, for the $\Delta D_o/D_o$ – κ response, the theoretical analysis by the endochronic theory combined with the principle of virtual work leads to the better simulation when compared with simulations by the finite element ANSYS, the finite element ABAQUS and experimental data.

REFERENCES

[1] Kyriakides, S. and Shaw, P. K., "Response and Stability of Elastoplastic Circular Pipes under Combined Bending and External Pressure," Int. J. Solids Struct., Vol. 18, No. 11, pp. 957-973, 1982.

[2] Shaw, P. K. and Kyriakides, S., "Inelastic Analysis of Thin-Walled Tubes under Cyclic Bending," Int. J. Solids Struct., Vol. 21, No. 11, pp.1073-1110, 1985.

[3] Kyriakides, S. and Shaw, P. K., "Inelastic Buckling of Tubes under Cyclic Loads," ASME J. Pres. Ves. Tech., Vol. 109, pp. 169-178, 1987.

[4] Corona, E. and Kyriakides, S., "On the Collapse of Inelastic Tubes under Combined Bending and Pressure," Int. J. Solids Struct., Vol. 24, pp. 505-535, 1988.

[5] Corona, E. and Kyriakides, S., "An Experimental Investigation Degradation and Buckling of Circular Tubes under Cyclic Bending and External Pressure," Thin-Walled Struct., Vol. 12, pp. 229-263,

1991.

[6] Corona, E. and Vaze, S., "Buckling of Elastic-plastic Square Tubes under Bending," Int. J. Mech. Sci., Vol. 38, No. 7, pp. 753-775, 1996.

[7] Vaze, S. and Corona, E., "Degradation and Collapse of Square Tubes under Cyclic Bending," Thin-Walled Struct., Vol. 31, pp. 325-341, 1998.

[8] Kyriakides, S. and Lee, L. H., "Buckle Propagation in Confined Steel Tubes," Int. J. Mech. Sci., Vol. 47, pp. 603-620, 2005.

[9] Corona, E., Lee, L. H., and Kyriakides, S., "Yield Anisotropic Effects on Buckling of Circular Tubes under Bending," Int. J. Solids Struct., Vol. 43, pp. 7099-7118, 2005.

[10] Kyriakides, S., Ok, A., and Corona, E., "Localization and Propagation of Curvature under Pure Bending in Steel Tubes with Lüders Bands," Int. J. Solids Struct., Vol. 45, pp. 3074-3087, 2006.

[11] Sakakibara, N., Kyriakides, S., and Corona, E., "Collapse of Partially Corrodes or Worn Pipe under External Pressure," Int. J. Mech. Sci., Vol. 50, pp. 1586- 1597, 2008.

[12] Pan, W. F., Wang, T. R., and Hsu, C. M., "A Curvature - Ovalization Measurement Apparatus for Circular Tubes under Cyclic Bending," Exp. Mech., Vol. 38, No. 2, pp. 99-102, 1998.

[13]Pan, W. F. and Fan, C. H., "An Experimental Study on the Effect of Curvature-rate at Preloading Stage on Subsequent Creep or Relaxation of Thin-walled Tubes under Pure Bending," JSME Int. J. (Japan Society of Mechanical Engineers), Series A, Vol. 41, No. 4, pp. 525-53, 1998.

[14] Pan, W. F. and Her, Y. S., "Viscoplastic Collapse of Thin-Walled Tubes under Cyclic Bending," ASME J. Eng. Mat. Tech., Vol. 120, pp. 287-290, 1998.

[15] Lee, K. L., Pan, W. F., and Kuo, J. N., "The Influence of the Diameter-to-thickness Ratio on the Stability of Circular Tubes under Cyclic Bending," Int. J. Solids Struct., Vol. 38, pp. 2401-2413, 2001.

[16] Lee, K. L., Pan, W. F., and Hsu, C. M., "Experimental and Theoretical Evaluations of the Effect between Diameter-to-thickness Ratio and Curvature-rate on the Stability of Circular Tubes under Cyclic Bending," JSME Int. J. (Japan Society of Mechanical Engineers), Series A, Vol. 47, No. 2, pp. 212-222, 2004.

[17] Chang, K. H., Pan, W. F., and Lee, K. L., "Mean Moment Effect of Thin-walled Tubes under Cyclic Bending," Struct. Eng. Mech. – an Int. J., Vol. 28, No. 5, pp. 495-514, 2008.

[18] Chang, K. H. and Pan, W. F., "Buckling Life Estimation of Circular Tubes under Cyclic Bending," Int. J. Solids Struct., Vol. 46, pp. 254-270, 2009.

[19] Gellin, S., "The Plastic Buckling of Long Cylindrical Shells under Pure Bending", Int. J. Solids Struct., Vol. 16, pp. 397-407, 1980.

[20] Valanis, K. C., "Fundamental Consequence of a New Intrinsic Time Measure-Plasticity as a Limit of the Endochronic Theory", Arch. Mech., Vol. 32, pp. 171-191, 1980.

[21] Pan, W. F., Lee, T. H., and Yeh. W. C., "Endochronic Analysis for Finite Elasto -plastic Deformation and Application to Metal Tube under Torsion and Metal Rectangular Block under Biaxial Compression", Int. J. Plasticity, Vol. 12, No. 10, pp. 1287-1316, 1996.

[22] Pan, W. F. and Chern, C. H., "Endochronic Description for Viscoplastic Behavior of Materials under Multiaxial Loading", Int. J. Solids Struct., Vol. 34, No. 17, pp. 2131-2159, 1997.

[23] Fan. J., "A comprehensive Numerical Study and Experimental Verification of Endochronic Plasticity", Ph.D. Dissertation, Department of Aerospace Engineering and Applied Mechanics, University of Cincinnati, 1983.